Robust Ce^{3+} valence across the pressure-driven collapse of magnetism in the frustrated Shastry-Sutherland compound Ce_2Pd_2In

P. Král [1,2,3,*] D. Staško [1] A. D. Rosa [4] E. Mijit [5] T. Irifune [6] J. Kaštil [2] L. Havela [1] and J. Prchal [1]

[1] *Charles University, Faculty of Mathematics and Physics, Department of Condensed Matter Physics, Ke Karlovu 5, Prague 121 16, Czech Republic*

[2] *Institute of Physics of the Czech Academy of Sciences, Na Slovance 1999/2, Prague 182 21, Czech Republic*

[3] *PSI Center for Neutron and Muon Sciences CNM, 5232 Villigen PSI, Switzerland*

[4] *ESRF, The European Synchrotron, 71 Avenue des Martyrs, CS40220, 38043 Grenoble Cedex 9, France*

[5] *Sorbonne Université, Muséum National d'Histoire Naturelle, UMR CNRS 7590, Institut de Minéralogie, de Physique des Matériaux et de Cosmochimie, Paris, France*

[6] *Premier Institute for Advanced Studies, Ehime University, Matsuyama, Ehime 790-8577, Japan*

(Received 20 May 2026; revised 22 July 2026; accepted 23 July 2026; published 17 August 2026)

Ce-based intermetallics often display a delicate interplay between magnetism, electron correlations, and lattice geometry, making them highly sensitive to external pressure. We report the evolution of the Ce valence in the frustrated Shastry-Sutherland compound Ce_2Pd_2In under high pressure using Ce L_3-edge x-ray absorption spectroscopy. Although long-range magnetic order collapses around ∼4 GPa, the spectra remain dominated by the the Ce $4f^1$ configuration across this region, pointing to its remarkable stability. Tiny signs of a valence increase appear only above ∼8 GPa, well beyond the pressure at which magnetism is suppressed. These observations demonstrate that the collapse of magnetic order is not driven by a valence instability but arises primarily from enhanced geometrical frustration within the Shastry-Sutherland lattice of Ce ions. Ce_2Pd_2In thus represents a rare realization of a Ce-based intermetallic in which frustration, rather than valence fluctuations, governs the suppression of long-range magnetic order, providing a clean platform to explore exotic ground states in frustrated rare-earth systems.

DOI: 10.1103/j1v2-4tcg

I. INTRODUCTION

Cerium-based intermetallic compounds often display rich pressure-dependent phase diagrams arising from the competition between Ruderman-Kittel-Kasuya-Yosida (RKKY) interactions, Kondo screening, and crystal electric field effects [1–4]. In many Ce systems, external pressure can additionally modify the Ce valence, driving a crossover from a localized Ce^{3+} configuration toward an intermediate-valence state [5–8], frequently accompanied by the suppression of magnetic order. More broadly, pressure-induced valence instabilities are also observed in other rare-earth systems. For example, Eu-based compounds exhibit pressure-driven transitions toward the nonmagnetic Eu^{3+} state [9], while in Yb systems pressure tends to stabilize the magnetic Yb^{3+} configuration [10–12], illustrating the strong sensitivity of rare-earth valence states to external pressure.

The compound Ce_2Pd_2In [13–15]—a member of the broad R_2T_2X family of intermetallics [16]—represents an interesting case within this context. It crystallizes in the tetragonal Mo_2FeB_2-type structure ($P4/mbm$), where Ce ions form a Shastry-Sutherland lattice [SSL, Fig. 1(a)], a geometry known to promote magnetic frustration, as seen in Yb_2Pt_2Pb [17,18] and Ce_2Pd_2Sn [19]. In such lattices, competing exchange interactions can lead to a manifold of nearly degenerate magnetic ground states, giving rise to complex magnetic phase diagrams [20–23] and an enhanced sensitivity to external parameters such as pressure.

Indeed, Ce_2Pd_2In exhibits unusual magnetic behavior: the ferromagnetic ground state ($T_C \approx 4.16$ K) is reached through an intermediate antiferromagnetic phase ($T_N \approx 4.65$ K) characterized by an incommensurate propagation vector. Recent transport measurements have shown that pressure initially stabilizes the antiferromagnetic phase at the expense of the low-temperature ferromagnetic phase, before ultimately suppressing long-range magnetic order above approximately 4 GPa [14,15]. Structural studies revealed that compression modifies the Ce-Ce distances within the basal plane, driving the system toward a configuration where nearly equilateral Ce triangles are formed. This evolution enhances magnetic frustration within the Shastry-Sutherland network and has been proposed as the key mechanism responsible for the eventual collapse of the antiferromagnetic order [15].

An alternative mechanism that may contribute to the suppression of magnetism is a pressure-induced modification of the Ce valence. In many Ce-based intermetallic

*Contact author: petr.kral@psi.ch

Published by the American Physical Society under the terms of the Creative Commons Attribution 4.0 International license. Further distribution of this work must maintain attribution to the author(s) and the published article's title, journal citation, and DOI.

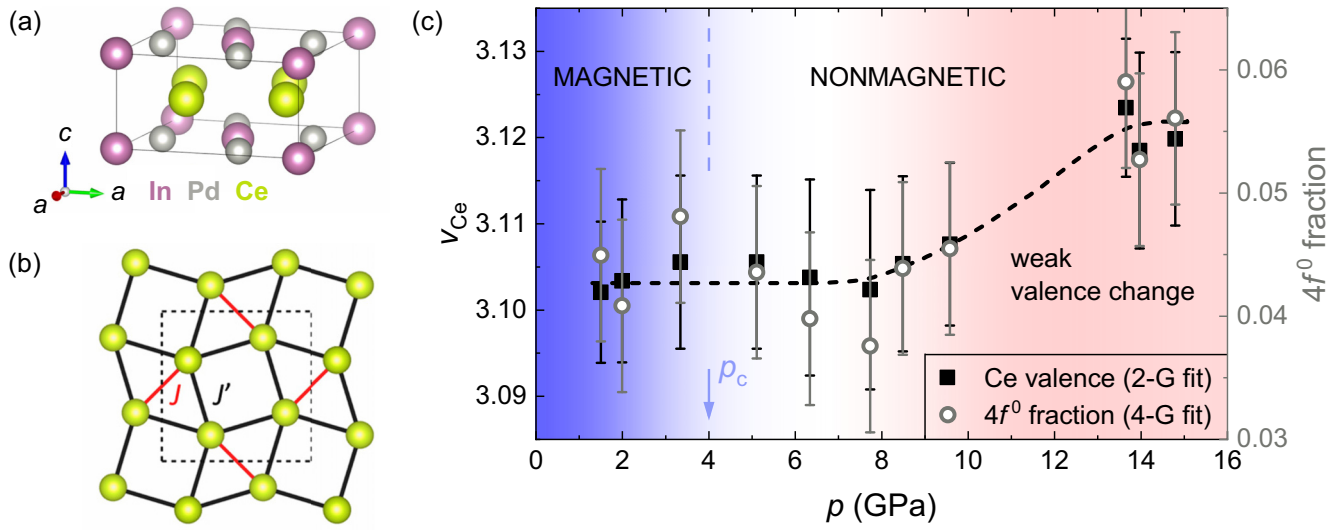


FIG. 1. Structural, magnetic, and electronic properties of Ce_2Pd_2In under pressure. (a) Ce_2Pd_2In unit cell and (b) Ce sublattice in the c-axis projection equivalent to the Shastry-Sutherland lattice (SSL) pattern. Shortest Ce-Ce distances (red) and second-shortest distances (black) are shown with corresponding exchange interactions J and J'. Compression enhances the equilateral character of the marked triangles, increasing frustration within the Shastry-Sutherland lattice. (c) Pressure phase diagram illustrating the evolution of the Ce valence under compression. Left axis: Ce valence from the two-Gaussian (2-G) decomposition of the XAS spectra (black square symbols). Right axis: relative fraction of the $4f^0$ component from four-Gaussian (4-G) fits (gray open-circle symbols). The Blue-white gradient marks the collapse of long-range magnetic order ($p_c \approx 4$ GPa, light-blue arrow) reported previously [15], without any detectable Ce valence change, while the white-red gradient highlights the region of a weak valence increase detected in XAS. The dashed line is guide to the eye.

compounds, lattice compression enhances the hybridization between the localized $4f$ electrons and the conduction band, which may lead to strengthened Kondo screening or a crossover toward an intermediate-valence state. Such a scenario frequently results in a gradual destabilization of the magnetic $4f^1$ configuration in favor of a nonmagnetic $4f^0$ state, with $4f^0$-$4f^1$ fluctuations eventually suppressing magnetic moments and long-range magnetic order. Since both mechanisms—enhanced geometrical frustration and pressure-induced valence instability—could potentially account for the collapse of magnetism in Ce_2Pd_2In, a direct probe of the Ce valence under pressure is therefore essential to clarify the origin of the observed behavior.

X-ray absorption spectroscopy (XAS) at the Ce L_3 ($2p_{3/2}$-$5d$ transition) edge provides a direct and highly sensitive probe of the Ce valence state through the distinct spectral signatures of the $4f^1$ and $4f^0$ electronic configurations, which are separated by approximately 11 eV. Performing such measurements under simultaneous high-pressure and low-temperature conditions, however, represents a significant experimental challenge, particularly because the Ce L_3 edge (~5.7 keV) lies in an energy range where absorption by the diamond anvils becomes substantial. Recent developments at the ESRF Extremely Brilliant Source (EBS), together with the high-flux capabilities of the ID24-DCM beamline, have now made such studies feasible [24].

In this work, we investigate the evolution of the Ce valence in Ce_2Pd_2In under lattice compression using high-pressure Ce L_3-edge x-ray absorption spectroscopy up to ≈15 GPa. The spectra remain dominated by the Ce $4f^1$ configuration across the pressure range where magnetic order collapses, with only weak signs of a valence increase appearing at higher pressures, indicating a generally robust trivalent Ce state. These results, summarized in Fig. 1(b), indicate that the collapse of magnetic order under pressure is primarily driven by enhanced magnetic frustration within the Shastry-Sutherland lattice, rather than a valence instability.

II. RESULTS

The Ce L_3-edge x-ray absorption spectra of Ce_2Pd_2In collected at 10 K are shown in Fig. 2(a). The spectra are dominated by the white line near 5722 eV, characteristic of the trivalent Ce $4f^1$ configuration. Across the pressures corresponding to the collapse of long-range magnetic order (~4 GPa), the spectral shape remains essentially unchanged, and no additional weight appears in the region associated with $4f^0$. This indicates that the Ce valence is remarkably stable in the pressure range where magnetism is suppressed.

To quantify this behavior, two complementary analyses were performed. In the first approach, a simple two-peak decomposition was applied, assigning the main peak to $4f^1$ and the higher-energy feature to $4f^0$, consistently for all pressures. The Ce valence [Fig. 1(c), left axis] was then estimated as

$$v = 3 + \frac{A_{4f^0}}{A_{4f^1} + A_{4f^0}}, \tag{1}$$

with A_{4f^1} and A_{4f^0} denoting the corresponding spectral weights.

The conventional two-Gaussian (2-G) analysis provides a phenomenological estimate of the average Ce valence. Since this simplified approach does not explicitly account for the weak $4f^2$ contribution and the asymmetric shape of the white line, the extracted absolute valence should be regarded as an approximate value. Nevertheless, because the same fitting procedure is applied consistently to all measured spectra, it

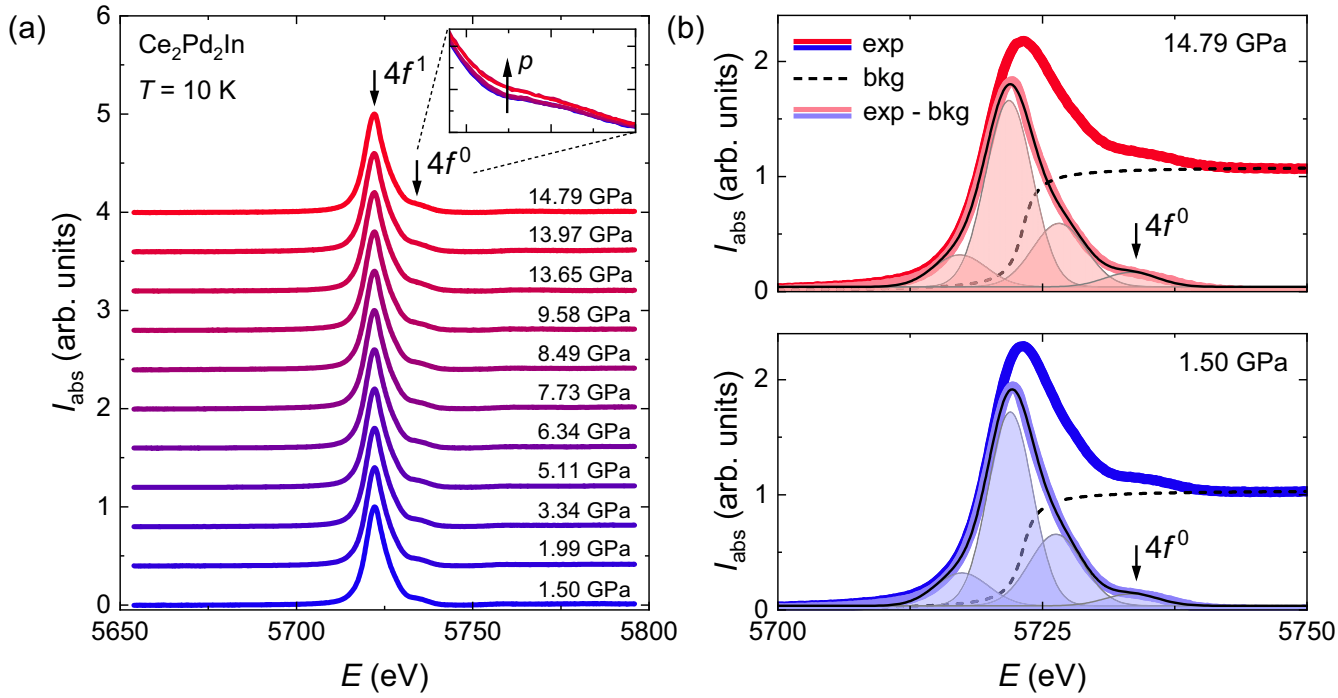


FIG. 2. Ce L_3-edge x-ray absorption spectra of Ce_2Pd_2In under pressure. (a) X-ray absorption spectra collected at 10 K under selected pressures. The main feature near 5722 eV corresponds to the trivalent Ce $4f^1$ state. No additional spectral weight associated with $4f^0$ is observed across the pressures corresponding to the collapse of magnetic order. The inset shows the higher-energy region around the $4f^0$ feature for all measured pressures, highlighting that the spectra remain nearly identical and overlap up to ∼8 GPa, while a subtle increase in the $4f^0$ intensity is observed for the three highest-pressure measurements. Spectra are normalized to the maximum of the main $4f^1$ peak. An arctangent background has been subtracted [see (b)]. (b) Representative fits of the lowest (1.50 GPa) and highest (14.79 GPa) pressure spectra using four Gaussian components ($4f^2$, $4f^1$, $4f^1_s$, $4f^0$, details in the main text) and an arctangent background (bkg).

reliably captures the pressure dependence of the $4f^0$ spectral weight.

To account for additional contributions to the XAS line shape, we additionally performed a four-Gaussian (4-G) decomposition of the spectra. Each spectrum was fitted using four Gaussian components, corresponding to $4f^2$, $4f^1$, a satellite $4f^1_s$ (associated with the main $4f^1$ peak), and $4f^0$, following methodologies reported in the literature [25,26]. The individual components capture the main electronic contributions, however, they also accommodate subtle deviations from ideal peak shapes. Even so, this approach provides a consistent way to track the relative fraction of the $4f^0$ component across all pressures, allowing for a qualitative comparison between spectra [Fig. 1(c), right axis]. Representative spectral fits at the lowest (1.50 GPa) and highest (14.79 GPa) pressures are shown in Fig. 2(b).

The phenomenological four-Gaussian decomposition is motivated by the microscopic description of Ce L_3-edge XAS within the single-impurity Anderson model (SIAM), commonly treated using the Gunnarsson-Schönhammer formalism [27,28] and its simplified implementation developed by Imer and Wuilloud [29]. Accounting for the final-state effects and the hybridization between the $4f$ and valence states, the model describes characteristic spectral features corresponding to different electronic configurations. The relative spectral weights and energy positions of individual contributions are governed by the parameters of the SIAM Hamiltonian, including the f-state energy, Coulomb repulsion, and hybridization strength. Considering parameter values characteristic of Ce compounds [25,27,29], the model yields a $4f^0$ satellite approximately 11 eV above the main line and a $4f^2$ component about 5 eV below it, in good agreement with our experimental observations, allowing us to assign the highest- and lowest-energy components of the four-Gaussian fit to the $4f^0$ and $4f^2$ configurations, respectively. The two central components of the fit correspond to the dominant $4f^1$ configuration.

The obtained spectral weights amount to ≈5% $4f^0$ and ≈10% $4f^2$ contributions, indicating a predominantly trivalent state. Compared with the two-component analysis, the explicit inclusion of the $4f^2$ contribution in the four-Gaussian decomposition redistributes part of the spectral weight from the main line to the $4f^2$ component, which would result in a lower estimated Ce valence. In contrast, the two-component analysis neglects the $4f^2$ contribution altogether, leading to a correspondingly higher estimate.

Importantly, both approaches confirm that the Ce valence remains essentially constant across the collapse of magnetism. At higher pressures, above ∼8 GPa, a subtle increase in the $4f^0$ contribution is observed in both the two-peak valence estimate and the $4f^0$ fraction from the four-Gaussian fits. The tendency for an increase of $4f^0$ peak intensity at the highest pressures is highlighted in the inset of Fig. 2(a), where all spectra are normalized to the main peak maximum. The corresponding curves nearly completely overlap up to ∼8 GPa, with only the highest-pressure spectra exhibiting a

subtle increase in the $4f^0$ intensity. The evolution of both the Ce valence and the $4f^0$ weight fraction are summarized in Fig. 1(c). Overall, the results demonstrate that the pressure-driven collapse of magnetic order in Ce_2Pd_2In occurs without a significant valence instability, with only minor changes developing at pressures well above the suppression of magnetism.

In addition, a small but systematic (linear) shift of the main $4f^1$ peak toward lower energy is observed with increasing pressure. The shift is weak (0.2 eV at $\approx$15 GPa), and is consistently captured by both the two-Gaussian and four-Gaussian analyses. It does not affect the overall spectral weight distribution between the $4f^1$ and $4f^0$ contributions. In Ce L_3-edge x-ray absorption spectroscopy, the $4f$ electrons do not participate directly in the $2p \rightarrow 5d$ excitation process. However, their occupancy influences the spectra via screening of the $2p$ core hole and the associated final-state energies. The observed shift is therefore consistent with a weak pressure-induced modification of the electronic environment and screening effects, without implying a change in Ce valence.

III. DISCUSSION

The present results demonstrate a pronounced stability of the trivalent Ce state in Ce_2Pd_2In over a wide pressure range. In particular, no detectable valence change occurs across the pressure where long-range magnetic order collapses ($\sim$4 GPa), with only subtle signs of valence increase appearing at higher pressures. This behavior contrasts with numerous Ce-based intermetallic compounds, where compression induces a partial or full $4f^1$ to $4f^0$ valence transition, often accompanied by the onset of Kondo screening and a suppression of magnetic order. For instance, $CeCu_2Si_2$ [5], $CeCu_2Ge_2$ [6], and $CePd_2Si_2$ [7] exhibit such pressure-driven valence instabilities, strongly affecting their magnetic and superconducting properties. Conversely, other Ce systems display only weak or delayed valence responses to pressure. For example, $CeRhIn_5$ shows a negligible valence change under moderate pressures despite the suppression of magnetism [30], similarly as the Ce valence in $CeRu_2Al_{10}$ [26] correlates only weakly with the corresponding critical disappearance of the antiferromagnetic order. These contrasting examples highlight the diversity of Ce valence responses to compression and place Ce_2Pd_2In among systems where the collapse of magnetism is not directly driven by a valence instability, pointing to a fundamentally different mechanism beyond the conventional Doniach phase diagram [1,3].

Previous studies on Ce_2Pd_2In have indicated an enhancement of Kondo correlations under pressure, associated with pressure-enhanced f-conduction electron hybridization [15]. However, the evolution of the magnetic ordering temperature does not follow the characteristic nonmonotonic behavior expected within the conventional Doniach scenario, where increasing exchange coupling first enhances and subsequently rapidly suppresses magnetic order. Instead, the monotonic suppression of $T_{C/N}$ suggests that additional mechanisms beyond the standard Doniach framework are relevant in this system. In this context, magnetic frustration—absent in the Doniach model—provides a natural channel for suppressing magnetic order [31,32]. As discussed previously [15], compression drives the Ce sublattice toward a network of nearly equilateral triangles, promoting the crossover from the Shastry-Sutherland regime toward more robust geometrical frustration. In this sense, magnetism can be destabilized already in a parameter range where it would still persist within the Doniach picture.

The observed stability of the Ce $4f^1$ configuration under pressure underscores the dominant role of geometrical frustration promoting strong competition among nearly degenerate magnetic states, which can destabilize long-range antiferromagnetic order even in the absence of significant valence fluctuations. Transport and structural studies indicate that magnetic order is suppressed above $\sim$4 GPa while the lattice retains the Shastry-Sutherland motif [15]. Our XAS measurements provide the missing microscopic evidence that Ce ions largely remain trivalent in this pressure range, confirming that enhanced frustration is sufficient to account for the observed collapse of magnetism, and the evolution of Kondo correlations and the suppression of magnetic order occur without entering the valence-fluctuation regime. Above $\sim$8 GPa, however, subtle signs of valence increase appear, indicating that while geometrical frustration is the primary driver of magnetic suppression, weak pressure-induced valence effects can emerge at higher pressures. The coexistence of weak pressure-induced electronic effects and magnetic frustration at elevated pressures underscores the unusual and delicate balance between lattice geometry and $4f$ electron behavior.

IV. CONCLUSION

In conclusion, high-pressure x-ray absorption spectroscopy of Ce_2Pd_2In provides direct microscopic evidence that the trivalent Ce $4f^1$ state remains largely stable up to $\approx$15 GPa, confirming that the collapse of long-range magnetic order at $\sim$4 GPa occurs without a significant change in Ce valence. Subtle signs of valence increase appear only at higher pressures, indicating that weak pressure-induced electronic effects emerge beyond the initial frustration-driven regime. Together with structural and transport data reported recently [15], these findings establish enhanced geometrical frustration within the Shastry-Sutherland lattice as the dominant mechanism governing the suppression of magnetic order. Ce_2Pd_2In therefore represents a rare and compelling example of a Ce-based intermetallic in which geometrical frustration, rather than valence instability, dominates the magnetic behavior under pressure. More broadly, these results provide a framework for exploring other frustrated Ce-based systems, where disentangling the roles of valence fluctuations and magnetic frustration is essential for understanding pressure-tuned magnetism and the emergence of exotic correlated ground states.

V. METHODS

High-pressure Ce L_3-edge x-ray absorption measurements were performed on polycrystalline Ce_2Pd_2In at the ID24-DCM beamline of the European Synchrotron Radiation Facility [24]—the beamline providing necessary high photon flux (low absorption energy and high absorbance of high-pressure sample environment), a highly focused beam ($0.7\times0.7\,\mu m^2$) to probe the micrometric sample in the

diamond anvil cell (DAC), and experimental setups optimized for high-pressure studies.

The sample was loaded into a membrane-driven DAC equipped with nanopolycrystalline diamond (NPD) anvils [33]—manufactured within the collaborative research project at GRC, Ehime University, Japan—to obtain the high-quality glitch-free data. On one diamond, a partially perforated NPD with Boehler-Almax design was mounted, while the opposite anvil consisted of a flat NPD mini-anvil placed on top of the fully perforated single-crystalline diamond. The NPDs with a culet diameter of 300 μm were used in both cases.

The Ce_2Pd_2In powder (the selected grains with the size in the order of ∼1 μm) was first pelletized (manually pressed in the DAC) to get a homogeneously abosrbing sample with a thickness of ≈5 μm required to obtain the optimal XAS signal. A small piece (20×20 μm in length and width) of the prepared pellet was then loaded into the DAC. As a pressure-transmitting medium, silicone oil was used. Although silicone oil can introduce nonhydrostatic stress at higher pressures, Ce L_3-edge x-ray absorption is a local probe and is only weakly sensitive to such effects. No stress-induced distortions of the spectral features are observed within experimental resolution. Pressure was determined using the ruby fluorescence [34], accounting also the temperature variations in the pressure calibration of the ruby spectrum.

The data [35] were collected at 10 K in the energy range 5710–5760 eV, covering the main $4f^1$ peak near 5722 eV and the region where a potential $4f^0$ contribution would appear (∼5734 eV), as well as the sufficiently extended pre- and post-edge part of the absorption spectrum, necessary for the proper analysis. The spectra were normalized using standard pre-edge and post-edge fitting procedures in the Larch software [36]. The $4f^1$ and $4f^0$ contributions were analyzed using conventional deconvolution methods (details in the main text).

Measurements at low temperatures were performed in a helium-flow high-pressure cryostat [24]. The diamond anvil cell is mounted directly within the first heat exchanger to ensure efficient thermal coupling. Temperature is monitored by thermocouples positioned near the sample region, allowing precise control during measurements. The vacuum vessel of the cryostat is equipped with circular x-ray-transparent Mylar windows.

ACKNOWLEDGMENTS

We acknowledge the European Synchrotron Radiation Facility (ESRF) for provision of synchrotron radiation facilities under proposal ID HC5533 on beamline ID24-DCM. We thank Dr. G. Garbarino for additional assistance during the beamtime. This work was supported by the Joint Usage/Research Center PRIUS, Ehime University, Japan. The project was further supported by the Grant Agency of Charles University (Project No. 358121) and the Czech Science Foundation (Grant No. 25-16339S). We further acknowledge MGML [37], which is supported within the program of Czech Research Infrastructures (Project No. LM2023065).

DATA AVAILABILITY

There are no publicly available research data or software supporting this manuscript. Requests for further information or data should be sent to the authors.

[1] S. Doniach, The Kondo lattice and weak antiferromagnetism, Physica B+C **91**, 231 (1977).

[2] J. S. Schilling, Electrical and magnetic properties of solids at high pressures: Some recent results, Physica B+C **139-140**, 369 (1986).

[3] B. Coqblin, M. D. Nunez-Regueiro, A. Theumann, J. R. Iglesias, and S. G. Magalhaes, Theory of the Kondo lattice: Competition between Kondo effect and magnetic order, Philos. Mag. **86**, 2567 (2006).

[4] H. v. Löhneysen, A. Rosch, M. Vojta, and P. Wölfle, Fermi-liquid instabilities at magnetic quantum phase transitions, Rev. Mod. Phys. **79**, 1015 (2007).

[5] J.-P. Rueff, S. Raymond, M. Taguchi, M. Sikora, J.-P. Itié, F. Baudelet, D. Braithwaite, G. Knebel, and D. Jaccard, Pressure-induced valence crossover in superconducting $CeCu_2Si_2$, Phys. Rev. Lett. **106**, 186405 (2011).

[6] H. Yamaoka, Y. Ikeda, I. Jarrige, N. Tsujii, Y. Zekko, Y. Yamamoto, J. Mizuki, J.-F. Lin, N. Hiraoka, H. Ishii, *et al.*, Role of valence fluctuations in the superconductivity of Ce122 compounds, Phys. Rev. Lett. **113**, 086403 (2014).

[7] H. Yamaoka, Y. Zekko, A. Kotani, I. Jarrige, N. Tsujii, J.-F. Lin, J. Mizuki, H. Abe, H. Kitazawa, N. Hiraoka, *et al.*, Electronic transitions in $CePd_2Si_2$ studied by resonant x-ray emission spectroscopy at high pressures and low temperatures, Phys. Rev. B **86**, 235131 (2012).

[8] Y. Cheng, R. He, Y. Xia, T. Han, L. Fang, S. Huang, and B. Liu, Sound velocities, and mechanical and electronic properties of the intermetallic compound $CeAl_2$ at high pressure, Phys. Rev. B **105**, 064106 (2022).

[9] C. Song, A. She, G. Xue, F. Yang, X. Bai, Y. Wang, Z. Hao, S. Zhang, and C. Cao, The valence states of europium in Eu-based intermetallic compounds: A review, Rev. Mater. Res. **2**, 100149 (2026).

[10] H. Yamaoka, A. Ohmura, N. Tsujii, H. Ishii, N. Hiraoka, H. Sato, and M. Sawada, Pressure-induced large valence transitions in Yb-Cu binary intermetallic systems, Phys. Rev. B **109**, 155147 (2024).

[11] R. S. Kumar, A. Svane, G. Vaitheeswaran, V. Kanchana, E. D. Bauer, M. Hu, M. F. Nicol, and A. L. Cornelius, Pressure-induced valence change in $YbAl_3$: A combined high-pressure inelastic x-ray scattering and theoretical investigation, Phys. Rev. B **78**, 075117 (2008).

[12] R. S. Kumar, A. Svane, G. Vaitheeswaran, Y. Zhang, V. Kanchana, M. Hofmann, S. J. Campbell, Y. Xiao, P. Chow, C. Chen, *et al.*, Pressure-induced valence and structural changes in $YbMn_2Ge_2$–Inelastic x-ray spectroscopy and theoretical investigations, Inorg. Chem. **52**, 832 (2013).

[13] M. Klicpera, S. Mašková, M. Diviš, P. Javorský, and L. Havela, Magnetic properties of Czochralski-grown Ce_2Pd_2In single crystal, J. Magn. Magn. Mater. **404**, 250 (2016).

[14] P. Král, J. Kaštil, M. Klicpera, P. Doležal, J. Prokleška, L. Havela, and J. Prchal, Stability of the $4f$-magnetism in Ce_2Pd_2In under hydrostatic and uniaxial pressure, J. Alloys Compd. **878**, 160304 (2021).

[15] P. Král, L. Havela, D. Staško, D. Daisenberger, M. Klicpera, M. Diviš, I. Puente-Orench, P. Proschek, J. Kaštil, M. Dopita, and J. Prchal, Kondo volume collapse in frustrated antiferromagnet: The case of Ce_2Pd_2In, Phys. Rev. Mater. **8**, 014401 (2024).

[16] M. Lukachuk and R. Pöttgen, Intermetallic compounds with ordered U_3Si_2 or Zr_3Al_2 type structure–Crystal chemistry, chemical bonding and physical properties, Z. Kristallogr. **218**, 767 (2003).

[17] M. S. Kim, M. C. Bennett, and M. C. Aronson, Yb_2Pt_2Pb: Magnetic frustration in the Shastry-Sutherland lattice, Phys. Rev. B **77**, 144425 (2008).

[18] P. Král, U. Dutta, J. Kaštil, M. Diviš, M. Míšek, P. Proschek, L. Havela, and J. Prchal, Crystal structure and magnetic properties of Yb_2Pt_2Pb under multi-extreme conditions, High Pressure Res. **44**, 479 (2024).

[19] J. G. Sereni, M. G. Berisso, A. Braghta, G. Schmerber, and J. P. Kappler, Unstable Shastry-Sutherland phase in Ce_2Pd_2Sn, Phys. Rev. B **80**, 024428 (2009).

[20] A. Ochiai, S. Matsuda, Y. Ikeda, Y. Shimizu, S. Toyoshima, H. Aoki, and K. Katoh, Field-induced partially disordered state in Yb_2Pt_2Pb, J. Phys. Soc. Jpn. **80**, 123705 (2011).

[21] Y. Shimura, T. Sakakibara, K. Iwakawa, K. Sugiyama, and Y. Ōnuki, Low temperature magnetization of Yb_2Pt_2Pb with the Shastry-Sutherland type lattice and a high-rank multipole interaction, J. Phys. Soc. Jpn. **81**, 103601 (2012).

[22] M. E. Zayed, C. Rüegg, J. Larrea J, A. M. Läuchli, C. Panagopoulos, S. S. Saxena, M. Ellerby, D. F. McMorrow, T. Strässle, S. Klotz, *et al.*, 4-spin plaquette singlet state in the Shastry-Sutherland compound $SrCu_2(BO_3)_2$, Nat. Phys. **13**, 962 (2017).

[23] T. Sakurai, Y. Hirao, K. Hijii, S. Okubo, H. Ohta, Y. Uwatoko, K. Kudo, and Y. Koike, Direct observation of the quantum phase transition of $SrCu_2(BO_3)_2$ by high-pressure and terahertz electron spin resonance, J. Phys. Soc. Jpn. **87**, 033701 (2018).

[24] A. D. Rosa, G. Garbarino, J. E. Rodrigues, E. Mijit, J. Jacobs, D. Bugnazet, S. Pasternak, G. Berruyer, A. Moyne, C. Clavel, *et al.*, New opportunities for high pressure x-ray absorption spectroscopy at ID24-DCM and BM23 with the extremely brilliant source of the ESRF, High Pressure Res. **44**, 248 (2024).

[25] H. Sato, T. Matsumoto, N. Kawamura, K. Maeda, T. Takabatake, and A. M. Strydom, Valence transition of the intermetallic compound Ce_2Rh_2Ga probed by resonant x-ray emission spectroscopy, Phys. Rev. B **105**, 035113 (2022).

[26] Y. Zekko, Y. Yamamoto, H. Yamaoka, F. Tajima, T. Nishioka, F. Strigari, A. Severing, J.-F. Lin, N. Hiraoka, H. Ishii, *et al.*, Correlation between the valence state of cerium and the magnetic transition in $Ce(Ru_{1-x}Fe_x)_2Al_{10}$ studied by resonant x-ray emission spectroscopy, Phys. Rev. B **89**, 125108 (2014).

[27] O. Gunnarsson and K. Schönhammer, Electron spectroscopies for Ce compounds in the impurity model, Phys. Rev. B **28**, 4315 (1983).

[28] O. Gunnarsson and K. Schönhammer, Double occupancy of the f orbital in the Anderson model for Ce compounds, Phys. Rev. B **31**, 4815 (1985).

[29] J.-M. Imer and E. Wuilloud, A simple model calculation for XPS, BIS and EELS $4f$-excitations in Ce and La compounds, Z. Phys. B **66**, 153 (1987).

[30] Z. E. Brubaker, R. L. Stillwell, P. Chow, Y. Xiao, C. Kenney-Benson, R. Ferry, Z. Jenei, R. J. Zieve, and J. R. Jeffries, Pressure dependence of Ce valence in $CeRhIn_5$, J. Phys.: Condens. Matter **30**, 035601 (2018).

[31] M. D. N. Regueiro, C. Lacroix, and R. Ballou, Effect of frustration near the magnetic-nonmagnetic transition, Phys. Rev. B **46**, 990 (1992).

[32] B. H. Bernhard, B. Coqblin, and C. Lacroix, Frustration in the Kondo lattice model: Local versus extended singlet phases, Phys. Rev. B **83**, 214427 (2011).

[33] T. Irifune, A. Kurio, S. Sakamoto, T. Inoue, and H. Sumiya, Ultrahard polycrystalline diamond from graphite, Nature (London) **421**, 599 (2003).

[34] M. I. Eremets, *High Pressure Experimental Methods* (Oxford University Press, Oxford, UK, 1996).

[35] P. Král, J. Prchal, and D. Staško, Pressure-induced valence changes as origin of magnetism loss in Ce_2Pd_2In, European Synchrotron Radiation Facility, https://doi.org/10.15151/ESRF-ES-1427751371.

[36] M. Newville, EXAFS analysis using FEFF and FEFFIT, J. Synchrotron. Radiat. **8**, 96 (2001).

[37] Materials Growth & Measurement Laboratory: Czech Open Access Research Infrastructure, https://mgml.eu/.